AD NUMBER

AD464786

LIMITATION CHANGES

TO:

Approved for public release; distribution is unlimited. Document partially illegible.

FROM:

Distribution authorized to U.S. Gov't. agencies and their contractors; Specific Authority; JUN 1965. Other requests shall be referred to Arnold Engineering Development Center, AFS, TN. Document partially illegible.

AUTHORITY

USAEDC ltr 16 Oct 1974

WIND TUNNEL INVESTIGATION OF FLEXIBLE AERODYNAMIC DECELERATOR CHARACTERISTICS AT MACH NUMBERS 1.5 TO 6

J. S. Deitering and E. E. Hilliard

ARO, Inc.

June 1965

VON KÁRMÁN GAS DYNAMICS FACILITY
ARNOLD ENGINEERING DEVELOPMENT CENTER
AIR FORCE SYSTEMS COMMAND
ARNOLD AIR FORCE STATION, TENNESSEE

NOTICES

When U.S. Government drawings specifications, or other data are used for any purpose other than a definitely related Government procurement operation, the Government thereby incurs no responsibility nor any obligation whatsoever, and the fact that the Government may have formulated, furnished, or in any way supplied the said drawings, specifications, or other data, is not to be regarded by implication or otherwise, or in any manner licensing the holder or any other person or corporation, or conveying any rights or permission to manufacture, use, or sell any patented invention that may in any way be related thereto.

Qualified users may obtain copies of this report from the Defense Documentation Center.

References to named commercial products in this report are not to be considered in any sense as an endorsement of the product by the United States Air Force or the Government.

Defense Documentation Center release to the Clearinghouse for Federal Scientific and Technical Information (CFSTI) and foreign announcement and distribution of this report are not authorized. The distribution of this report is limited because it contains technology identifiable with items excluded from export by the Department of State.

WIND TUNNEL INVESTIGATION OF FLEXIBLE AERODYNAMIC DECELERATOR CHARACTERISTICS AT MACH NUMBERS 1.5 TO 6

J. S. Deitering and E. E. Hilliard
ARO, Inc.

FOREWORD

The work reported herein was done at the request of the Air Force Flight Dynamics Laboratory (AFFDL), Air Force Systems Command (AFSC), for the Tech-Center Division of the Cook Electric Company and for the Goodyear Aerospace Corporation under Program Element 62405364/6065, Task 606505.

The results of tests presented were obtained by ARO, Inc. (a subsidiary of Sverdrup and Parcel, Inc.), contract operator of the Arnold Engineering Development Center (AEDC), AFSC, Arnold Air Force Station, Tennessee, under Contract AF40(600)-1000. The tests were conducted from November 9, 1964 to March 6, 1965 under ARO Project No. VT0515, and the report was submitted by the authors on May 12, 1965.

This technical report has been reviewed and is approved.

Darreld K. Calkins
Major, USAF
AF Representative, VKF
DCS/Test

Jean A. Jack
Colonel, USAF
DCS/Test

ABSTRACT

Tests were conducted in the 40-in. supersonic Tunnel A of the von Kármán Gas Dynamics Facility to investigate the drag and stability characteristics of a series of flexible decelerator models. The models were tested at Mach numbers from 1.5 to 6 at dynamic pressures corresponding to pressure altitudes of 75,000 to 135,000 ft, respectively. Four basic decelerator configurations were examined: hyperflo parachutes at variable locations aft of three forebody models, hemisflo parachutes with varied amounts of canopy inlet reefing, a tandem configuration composed of a hyperflo parachute inside the suspension lines of a hemisflo parachute, and a conical ballute decelerator.

CONTENTS

ILLUSTRATIONS

TABLES

NOMENCLATURE

a	Parachute canopy skirt length, in.
C_D	Drag coefficient of ballute decelerator based on projected surface area excluding the fence, drag force/$q_\infty S_p$
C_{D_o}	Drag coefficient of parachute canopy based on total surface area, drag force/$q_\infty S_o$
C_{D_p}	Drag coefficient of parachute canopy based on projected canopy area, drag force/$q_\infty S_p$
D_i	Parachute canopy inlet diameter, in.
D_m	Parachute roof screen diameter, in.
D_o	Reference diameter, equal to $(4S_o/\pi)^{1/2}$, in.
D_p	Inflated decelerator projected diameter, in.
D_v	Parachute canopy vent diameter, in.
d	Forebody base diameter, in.

ℓ_S	Length of parachute suspension lines, in.
M_∞	Free-stream Mach number
p_i	Ballute internal pressure, psia
p_∞	Free-stream static pressure, psia
q_∞	Free-stream dynamic pressure, psia
S_p	Design projected area of inflated decelerator, in.^{2}
S_o	Total parachute canopy surface area including slots and vent, in.^{2}
s	Surface length, in.
w	Parachute canopy radial ribbon width, in.
x	Distance from the base of the forebody model to the ballute or parachute canopy inlet, in.
λ_t	Total parachute canopy porosity, percent
ξ	Parachute canopy inlet reefing ratio (ratio of reefed inlet area to fully inflated inlet area)

SECTION I
INTRODUCTION

The purpose of this investigation was to provide data for the determination of the effects of construction variables on the performance of certain flexible aerodynamic decelerators known to possess good retardation, inflation, and stability characteristics in supersonic flow regimes. A total of 23 decelerator configurations were examined in the 40-in. supersonic tunnel (Gas Dynamic Wind Tunnel Supersonic (A)), von Kármán Gas Dynamics Facility (VKF), AEDC, AFSC. These consisted of hyperflo- and hemisflo-type parachutes and one Goodyear conical ballute decelerator. Except for one configuration which was a combination of a hyperflo parachute inside a hemisflo parachute, all configurations tested were single decelerators. In addition to the construction variables, the locations of the hyperflo parachute model aft of the forebody models were varied, and the hemisflo parachutes were tested at several inlet reefing conditions.

The decelerator models were tested at Mach numbers from 1.5 to 6 at dynamic pressures corresponding to pressure altitudes of 75,000 to 135,000 ft, respectively. The performance characteristics obtained included decelerator drag, inflation, and stability. Stability characteristics as discussed in this report refer only to the conditions of oscillatory motion of each decelerator with respect to the forebody model.

The test program also included a wake survey investigation at M_∞ = 2 to 5 in which local pitot and static pressure measurements were made in vertical traverses at various stations aft of the forebody models. These data will be utilized by the users (Cook Electric Company) in the analysis of parachute performance, and no presentation is made herein.

SECTION II
APPARATUS

2.1 WIND TUNNEL

Tunnel A is a continuous, closed-circuit, variable density wind tunnel with an automatically driven flexible plate-type nozzle and a 40- by 40-in. test section. The tunnel operates at Mach numbers from 1.5 to 6 at maximum stagnation pressures from 29 to 200 psia, respectively, and stagnation temperatures up to 300°F (M_∞ = 6). Minimum operating

pressures are about one-tenth of the maximum at each Mach number. A description of the tunnel and airflow calibration information may be found in the Test Facilities Handbook. *

2.2 TEST ARTICLES

2.2.1 Parent Models and Support Systems

The parachute decelerator models were investigated in the wakes of three models which, by means of a tapered strut common to each, were mounted to the tunnel sidewall in the upstream region of the test section. Sketches of the strut geometry and tunnel installation are given in Figs. 1a and b, respectively. The forebody models consisted of a sharp cone-cylinder (I), a blunt cone-cylinder-flare (II), and a spherically blunted cylinder (III). Sketches of the three forebody geometries are given in Fig. 1c.

The parachute models were tested behind each of the three forebodies. The models were attached to a swivel from which a line was routed through the forebody and strut to a winch assembly. In the case of the hyperflo parachutes this winch assembly allowed the parachutes to be moved to various stations (x/d) aft of the parent body.

The conical ballute decelerator was tested behind a parent body (forebody configuration IV), a spiked cone-cylinder body with a flare-cylinder afterbody. The ballute model, unlike the parachutes, was attached by a support line directly to the forebody model. The dimensions of this forebody and strut are given in Fig. 2.

2.2.2 Decelerator Models

The decelerators tested consisted of three general types: hyperflo parachutes, hemisflo parachutes, and a conical, inflatable balloon (ballute). A fourth type, the combination of a small hyperflo parachute inside the suspension lines of a larger hemisflo parachute, was also tested. Photographs and construction details of these decelerators are presented in Figs. 3 through 7.

---

*Test Facilities Handbook (Fifth Edition). "von Kármán Gas Dynamics Facility, Vol. 4." Arnold Engineering Development Center, July 1963.

2.2.2.1 Hyperflo Parachutes

The hyperflo parachutes were characterized by a truncated cone design with flat, porous roofs and solid-cloth, low-porosity skirts. The typical hyperflo parachute construction is presented in Fig. 4a, and design specifications for each configuration are given in Fig. 4b. Principal construction variables were canopy projected diameter (D_p), canopy total porosity (λ_t), and screen material employed in the roofs. Canopy diameters of the test parachutes were 3, 5, 6.8, and 8.2 in., and canopy total porosity varied from 5 to 20 percent. Canopy suspension line length was equal to twice the canopy diameter in all cases. Canopy location (x/d) aft of the three parent bodies was varied from 3.5 to 16. A total of 17 hyperflo parachute configurations were investigated.

2.2.2.2 Hemisflo Parachutes

Hemisflo parachutes are shaped-gore ribbon parachutes; that is, the canopies are constructed in the shape that they will normally assume when inflated in supersonic flow. The canopy of the hemisflo parachute is constructed as a hemisphere with a skirt extension added between suspension lines. These characteristics are shown in Fig. 5, which presents construction details. Two sizes of the hemisflo parachute were tested, and the reference diameters (D_o) were 13 and 21.33 in. Total porosity for the 13-in. hemisflo parachute canopy was 14.1 percent and ranged from 9.4 to 18 percent for the 21.33-in. canopy. Canopy inlet reefing was varied during testing of the hemisflo parachute configurations. The reefing line technique used for this purpose is illustrated in Fig. 6. A total of five hemisflo parachute configurations were tested.

2.2.2.3 Tandem Parachute

One configuration of the tandem parachute was tested. This configuration consisted of two complete parachutes- a hyperflo parachute (D_p = 3 in.) inside the suspension lines of the 13-in.-diam hemisflo parachute (ℓ_s = 21.6 in.). Both parachutes are described individually in Figs. 4 and 5 according to their type. Figure 5 shows the hyperflo parachute inside the hemisflo parachute suspension lines.

2.2.2.4 Ballute Decelerator

One configuration of a ballute decelerator was tested. This was a 75-deg, cone-sphere balloon constructed of eight equal gores of nonporous, rubber-coated nylon cloth. The diameter at the equator of the spherical portion was 7.0 in. A burble fence located around the equator increased the diameter of the ballute by 0.88 in. The ballute was inflated by ram air pressure through four diametrically opposed, forward facing

inlets. Internal pressure in the ballute was measured during testing. Model dimensions are given in Fig. 7.

2.3 INSTRUMENTATION

Two high-speed 16-mm motion-picture cameras, two cameras for still photography (regular and schlieren), and an oscillograph for recording a time history of the dynamic drag output from a tensiometer were used to record parachute performance. One movie camera operating at approximately 500 fps recorded side views of the parachutes; the other, operating at approximately 1000 fps, was installed in the tunnel schlieren system.

Three tensiometers located in the winch assembly outside the tunnel - rated at 200, 300, and 600 lb - were used to measure hemisflo parachute reefing line loads, hyperflo parachute drag loads, and hemisflo parachute drag loads, respectively. Forebody IV was equipped with a 600-lb tensiometer to measure the drag of the ballute decelerator model. The drag data obtained from the tensiometers located in the winch assembly are estimated to be accurate to within 6 percent based on the repeatability obtained in the calibration loadings. Some hysteresis was found in the calibration results from the combined effects of friction in the pulley systems inside the forebodies and the stretching under tension of the long nylon parachute support lines.

The ballute internal pressure was measured with a 15-psid transducer, referenced to a near vacuum, having full-scale calibrated ranges of 1, 5, and 15 psia. These pressure measurements are considered accurate to within 0.2 percent of full scale for each range.

SECTION III
TEST PROCEDURE

Before each test run the parachute canopy and suspension lines were packed in a deployment bag. The bag was then suspended near the base of the forebody model by a pull cord routed from the rear of the bag through the tunnel sector. The pull cord was held taut manually during tunnel start and until the desired test condition was established, when a sharp pull on the cord removed the bag. Parachute location and reefing ratio were set by a remotely operated winch assembly. Normal on-line tunnel Mach number changes and tunnel pressure level adjustments were made with the parachute still deployed.

For the ballute model no deployment bag was used, but the model was suspended in the tunnel by the pull cord tied to the model base. After tunnel flow was established, the pull cord was simply slackened to remove the effect of the cord tension on the ballute performance.

Summaries of the program, main test conditions, and results obtained for the various decelerator configurations are given in Tables I through IV. The drag coefficients presented in these tables were obtained by averaging the drag from the individual dynamic drag traces. The observations given in the tables are the results of evaluations of the photographic data and drag traces.

SECTION IV
RESULTS AND DISCUSSION

4.1 HYPERFLO PARACHUTES

Sixteen parachutes of the hyperflo type were tested at dynamic pressures corresponding to pressure altitudes of 83,000 ft at $M_\infty = 2$ to 149,000 ft at $M_\infty = 5.5$. In addition to variations in canopy size, total porosity, and type of roof material, the influences of forebody shape and x/d location on the stability and drag of these parachutes were also investigated. The summary of the hyperflo parachute test conditions and results is presented in Table I. All configurations were tested behind one or more of forebody configurations I through III.

In general, the drag coefficients for the hyperflo parachutes decreased with increasing Mach number and decreasing location (x/d) aft of the forebody model. Since only a limited amount of drag data was obtained at identical x/d's for each of the three forebodies for any one parachute configuration, direct comparisons of drag with forebody model variation are limited. Typical drag results for three hyperflo parachutes, which differ only in total canopy porosity, in the wakes of forebodies I and II are presented in Fig. 8. The increase in drag produced by the decrease in canopy porosity was small at Mach numbers from 2 to 5.5. Drag coefficients for hyperflo configurations 2 and 3 behind forebody II were very low at $M_\infty = 4$, 5, and 5.5 for x/d's of 3 to 4. With the parachutes at these locations, the forebody wake opened up (diverged), and a major portion of the parachute was enclosed in a large region of low-energy flow. This resulted in a very stable parachute with underinflation and low drag. At $M_\infty = 4$, 5, and 5.5, it was generally found that the canopy location required to open the wake moved downstream slightly with increasing Mach number and with decreasing free-stream dynamic pressure at each Mach number.

The effect of canopy diameter on drag is presented in Fig. 9 for the perlon mesh-roofed hyperflo parachutes of 15-percent porosity (configurations 1, 5, and 8) in the wake of forebody II at M_∞ = 4, 5, and 5.5. The data at M_∞ = 5 and 5.5 for configuration 8 at x/d = 6 show that the larger diameter chute had a greater influence in causing the wake to open up. The data at M_∞ = 4 and 5 for configuration 8 at x/d = 6 and at M_∞ = 5 and 5.5 for configuration 5 at x/d = 5.5 show that the parachute x/d location at which the forebody wake opened moved downstream with increasing Mach number.

Inflation characteristics of the hyperflo parachute were generally very good. Most of the underinflation observed occurred with the parachute towed close to the forebody in the open-wake conditions mentioned above. Stability of the hyperflo parachutes, although dependent upon many factors besides x/d location, appeared to be better overall at x/d < 8 with forebody I and at x/d < 5 with forebodies II and III.

4.2 HEMISFLO PARACHUTES

Five hemisflo-type parachutes were tested in the Mach number range from 1.5 to 3 at dynamic pressures corresponding to pressure altitudes of 75,000 to 118,000 ft, respectively. All but one of the hemisflo parachutes were tested with varied amounts of canopy inlet reefing. All five configurations were tested in the wake of forebody I. The parachute configurations and the results of the tests are summarized in Table II.

The 13-in.-diam hemisflo parachute with the short suspension lines (ℓ_S = 11.7 in.) was reasonably stable at M_∞ = 3 but very unstable at M_∞ = 2 and 2.5 with much pulsing of the canopy. A similar chute with ℓ_S = 21.6 in. exhibited very good inflation and stability characteristics at almost all test conditions from M_∞ = 1.5 to 3. This parachute is shown in Fig. 10 along with the drag coefficients (C_{D_o}) obtained over the reefing ratio range at each Mach number.

4.3 TANDEM PARACHUTE

One configuration of the tandem-type parachute was tested at M_∞ = 2 and 3 at dynamic pressures corresponding to pressure altitudes of 91,000 and 118,000 ft, respectively. This configuration consisted of a 3-in.-diam hyperflo parachute positioned inside the suspension lines of a 13-in.-diam hemisflo parachute (ℓ_S = 21.6 in.). The hemisflo parachute was not reefed, and its position was fixed at x/d = 10.6; the

hyperflo parachute locations aft of the forebody were varied from x/d = 4.0 to 7.25. The test results are presented in Table III.

4.4 BALLUTE DECELERATOR

The conical ballute decelerator was tested at Mach numbers from 4 to 6 at dynamic pressures corresponding to pressure altitudes of 102,000 to 135,000 ft, respectively. The ballute was towed at an x/d of 9 in the wake of forebody configuration IV. In addition to drag, inflation, and stability data as obtained with the parachutes, internal ballute pressures were obtained at all test conditions for the purpose of providing structural design information. The test conditions and results obtained are presented in Table IV.

As noted in the table, the ballute model was very stable (no coning or roll) and well inflated at each Mach number and dynamic pressure level. The drag coefficients and internal pressure recovery ratios for all test conditions are given in Fig. 11.

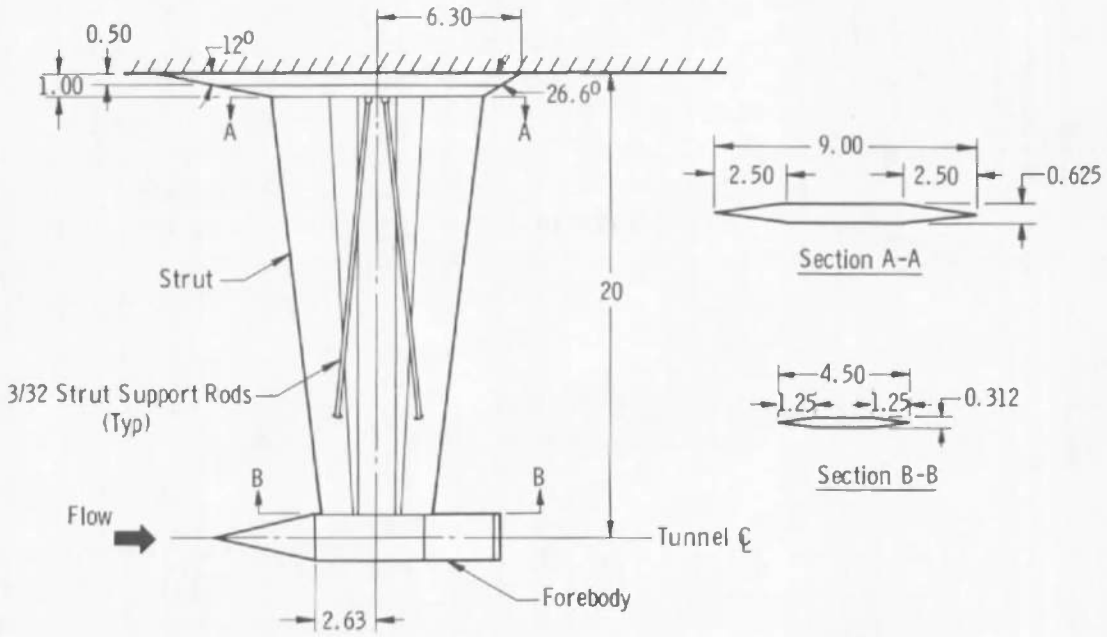

a. Forebody Strut Details

All Dimensions in Inches

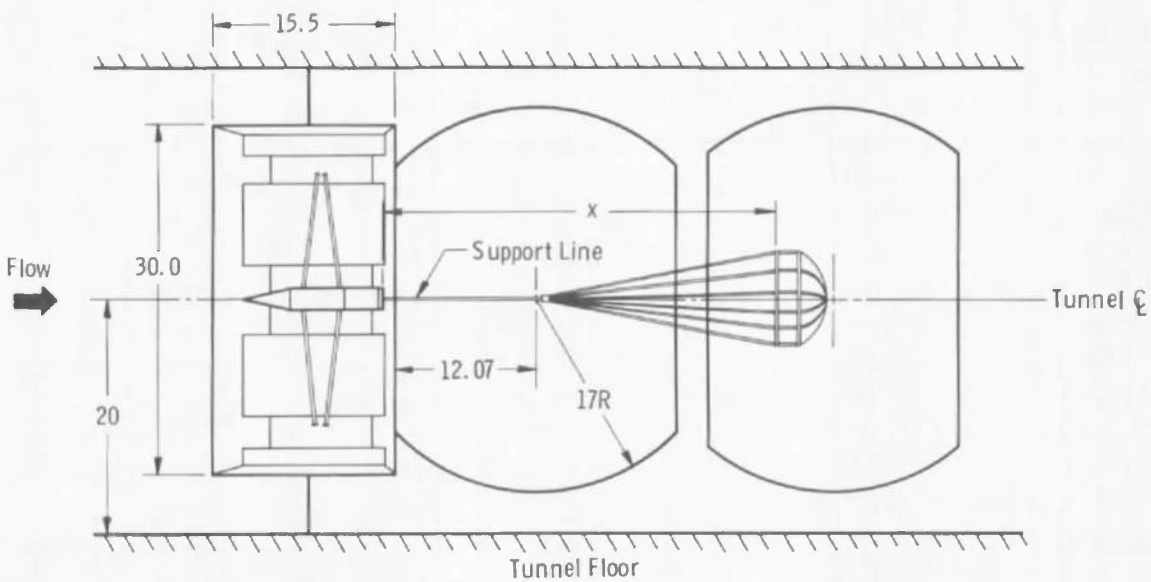

b. Tunnel Installation Sketch

Fig. 1 Forebody and Strut Support for the Hyperflo and Hemisflo Parachutes

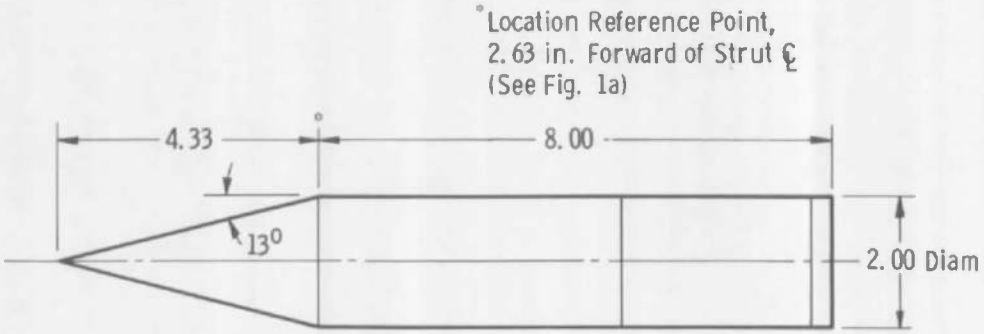

Forebody Configuration I

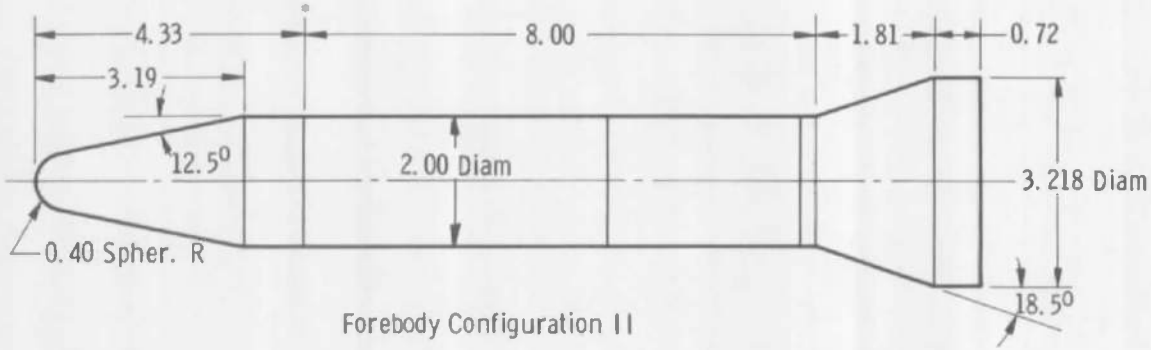

Forebody Configuration II

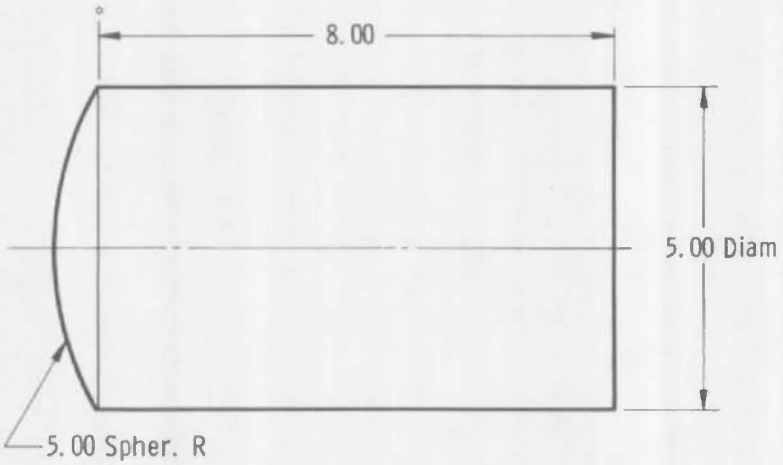

Forebody Configuration III

c. Forebody Details

Fig. 1 Concluded

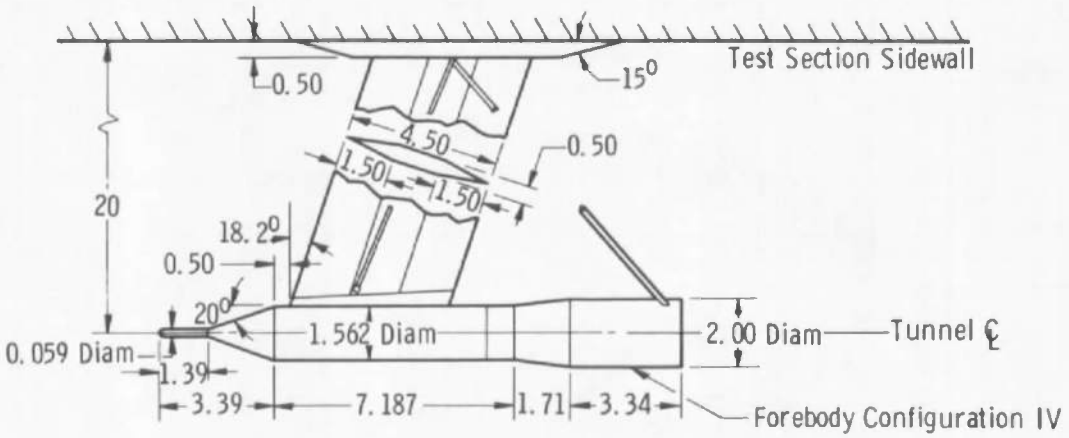

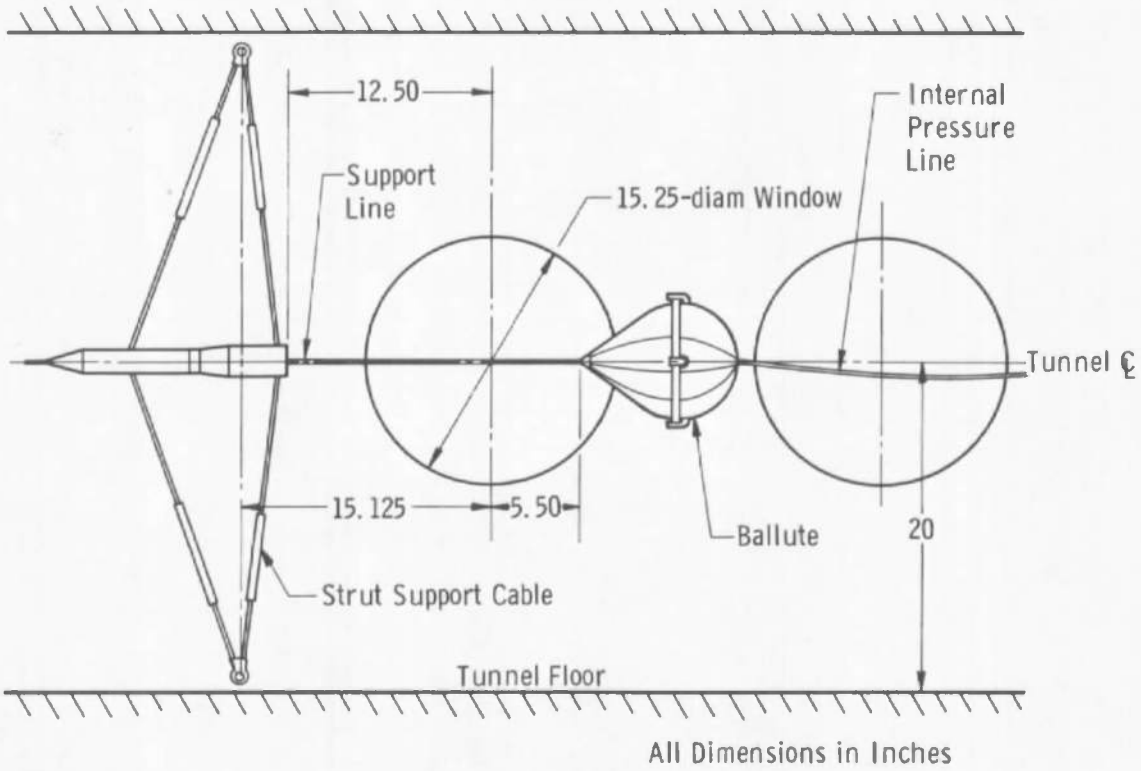

Fig. 2 Forebody and Strut Support for the Ballute Tests

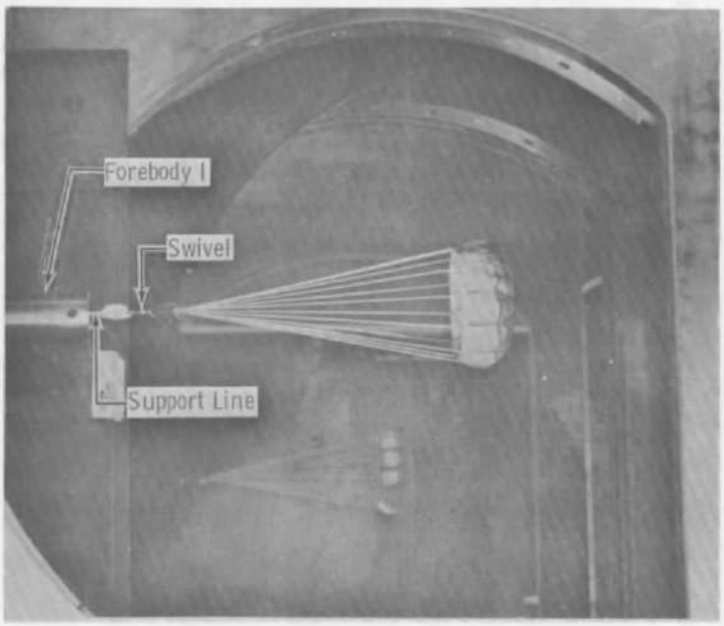

Hyperflo Configuration 2, $M_\infty = 3$

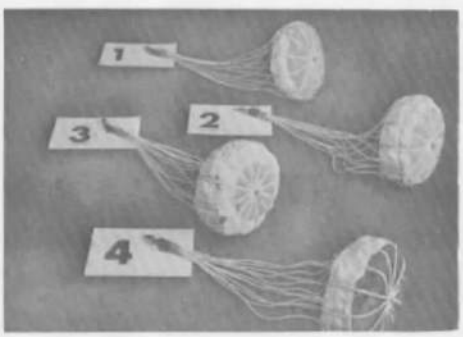

Hyperflo Porochutes

Numbers Refer to Configurations (See Figs. 4 and 5 and Tables I and II)

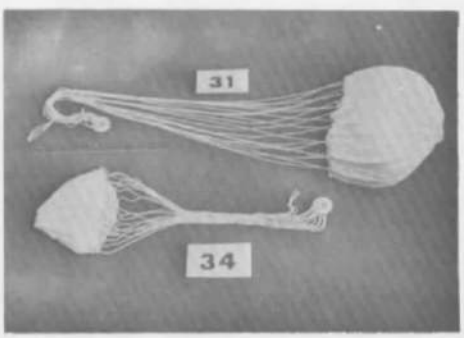

Hemisflo Porochutes

Fig. 3 Photographs of Hyperflo and Hemisflo Parachutes

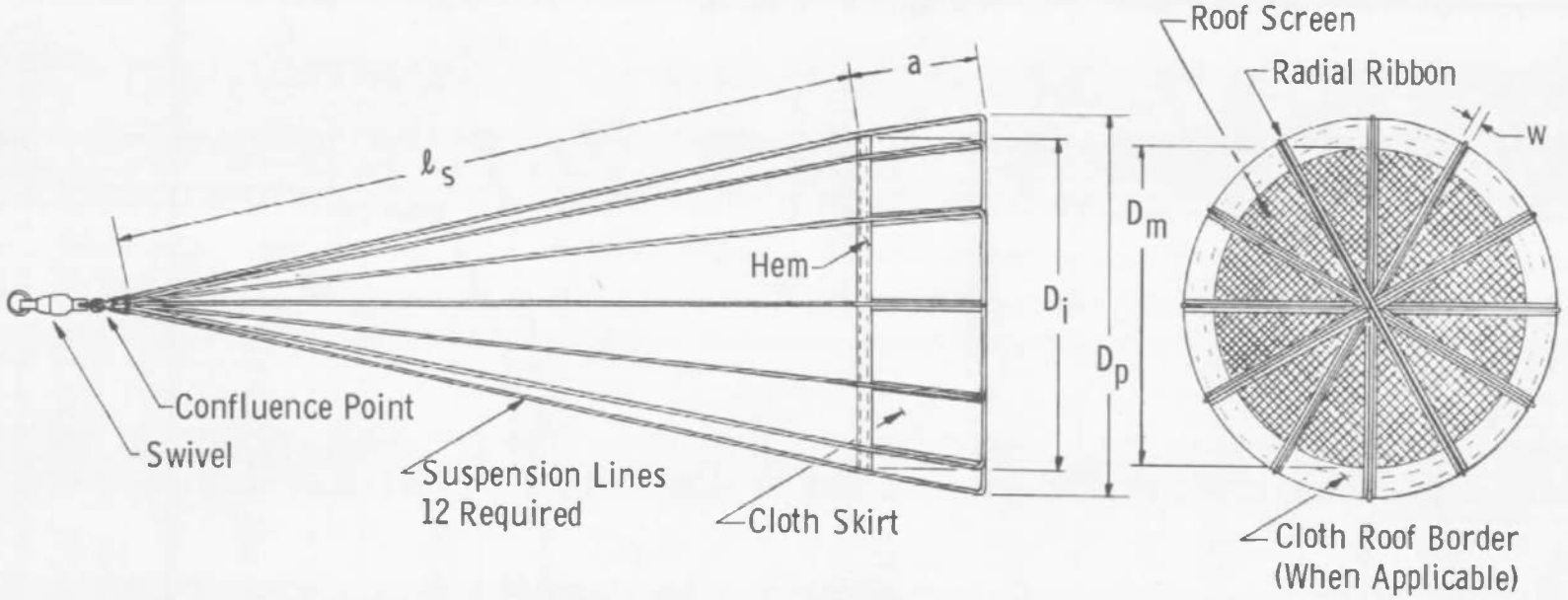

a. Typical Hyperflo Construction

Fig. 4 Hyperflo Parachute Construction and Design Specifications

Config. Number	λ_t, percent	D_p, in.	D_m, in.	D_i, in.	a, in.	ℓ_s, in.	Suspension Line Material	Skirt Material	Roof Border and Radial Ribbon Material	Roof Screen Material	w, in.
1	15	5.00	4.78	4.50	1.44	10.00	Cord, nylon 100-lb Mil-C-5040, Type 1	Cloth, nylon 300-lb/in. Mil-C-8021, Type 2	Neoprene-coated nylon Dantex® 5678	Perlon mesh 25/2/280, 64 by 64 Grid (per in.)	0.15
2	10	5.00	3.98	4.50	1.44	10.00	↑	↑	↑	↑	0.15
3	5	5.00	2.90	4.50	1.44	10.00	↑	↑	↑	↑	0.15
4	20	5.00	4.92	4.50	1.44	10.00	↑	↑	↑	Nylon knit No. 100022, 12-1/2 by 11 Grid	0.15
5	15	6.80	6.62	6.12	1.96	13.60	↑	Cloth, Nomex HT-67	↑	Perlon mesh 25/2/280, 64 by 64 Grid	0.21
8	15	8.20	7.98	7.38	2.36	16.40	↑	↑	↑	↑	0.25
9	10	8.20	6.04	7.38	2.36	16.40	↑	↑	↑	Nylon knit No. 100022, 12-1/2 by 11 Grid, 100-lb cord mesh	0.25
10	5	8.20	7.30	7.38	2.36	16.40	↑	↑	↑	↑	0.25
12*	15	3.00	2.76	2.70	0.87	6.00	Nylon 90-lb Braided Fishing Line	Cloth, nylon 200-lb/in. Mil-C-8021, Type 1	↑	Perlon mesh 25/2/280, 64 by 64 Grid	0.06
13	10	8.20	6.68	7.38	2.36	16.40	Cord, nylon 100-lb	Cloth, Nomex	↑	↑	0.25
14	10	8.20	7.76	7.38	2.36	16.40	Mil-C 5040, Type 1	HT-67	↑	Perlon mesh Monodur 80, 160 by 160 Grid	0.25
15	5	8.20	4.98	7.38	2.36	16.40	↑	↑	↑	Perlon mesh 25/2/280, 64 by 64 Grid	0.25
17	15	5.00	5.00	4.50	1.44	10.00	↑	Cloth, nylon 300-lb/in. Mil-C-8021, Type 2	N/A	Nomex ribbon No. 9759, 0.115 in., 4 by 4 Grid	0.25
18	10	5.00	4.78	4.50	1.44	10.00	↑	↑	Neoprene-coated nylon Dantex 5678	Nomex ribbon No. 9759, 0.132 in., 3.5 by 3.5 Grid	0.15
19	5	5.00	3.46	4.50	1.44	10.00	↑	↑	↑	Nomex ribbon No. 9759,	0.15
21	10	5.00	5.00	4.50	1.44	10.00	↑	↑	N/A	0.07 in., 7-3/4 by 7-3/4 Grid	0.08
22	10	5.00	4.76	4.50	1.44	10.00	↑	↑	Neoprene-coated nylon Dantex 5678	Nylon ribbon, Mil-R-5608, Class C, Type 1, 1/4 in. 39-lb, 2-1/4 by 2-1/4 Grid	0.15

*Configuration 12 was tested only as part of Conf. 35 (see Fig. 5 and Table III).

b. Hyperflo Design Specificotions

Fig. 4 Concluded

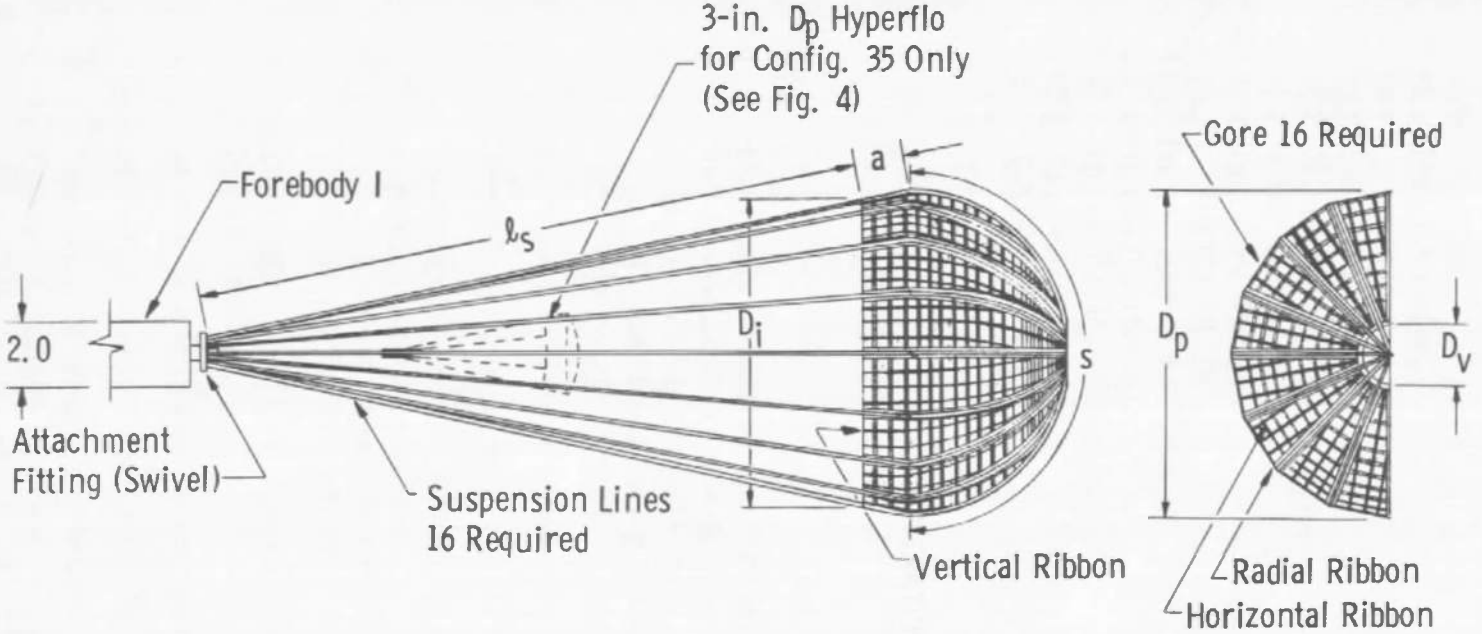

Config. Number	D_o, in.	λ_t, percent	D_p, in.	D_i, in.	ℓ_s, in.	a, in.	D_v, in.	Horizontal and Radial Ribbon Material	Vertical Ribbon Material	Suspension Line Material	Distance between Vertical Ribbons, in.	Distance between Horizontal Ribbons, in.	Number of Horizontal Ribbons per Gore	Number of Vertical Ribbons per Gore	s, in.
31	21.33	14.58	13.19	12.57	37.97	2.095	2.52	Ribbon, Nylon Mil-R-5608, Class C, Type 1, 1/4 in., 39 lb	Nomex Ribbon No. 9759, 0.07 in.	Cord, nylon Mil-C-5040, Type 1, 100 lb	0.53	0.0356	39	3	20.95
32	"	17.95	"	"	"	"	"				"	0.0515	37	"	"
33	"	9.35	"	"	"	"	"				"	0.0147	42	"	"
34	13.00	14.14	8.04	7.66	21.61	1.28	1.74		Nomex Ribbon No. 9759, 0.132 in.		N/A	0.0425	23	1	12.77
35*	"	"	"	"	"	"	"				"	"	"	"	"
36	"	"	"	"	11.70	"	"				"	"	"	"	"

*Same as Config. 34 but with 3-in. D_p hyperflo inside suspension lines.

Fig. 5 Hemisflo Parachute Construction and Design Specifications

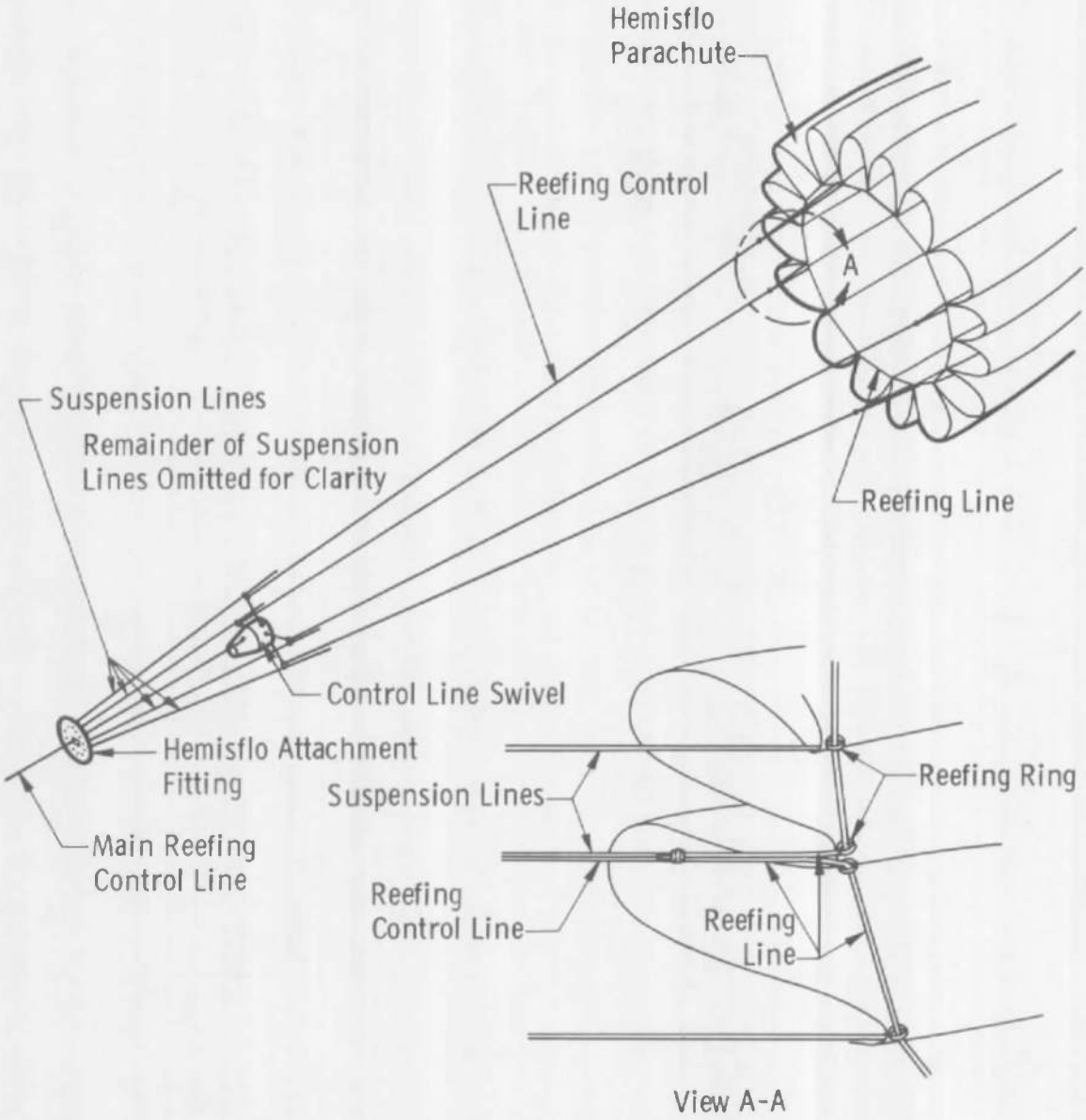

Fig. 6 Sketch of Hemisflo Canopy Inlet Reefing System

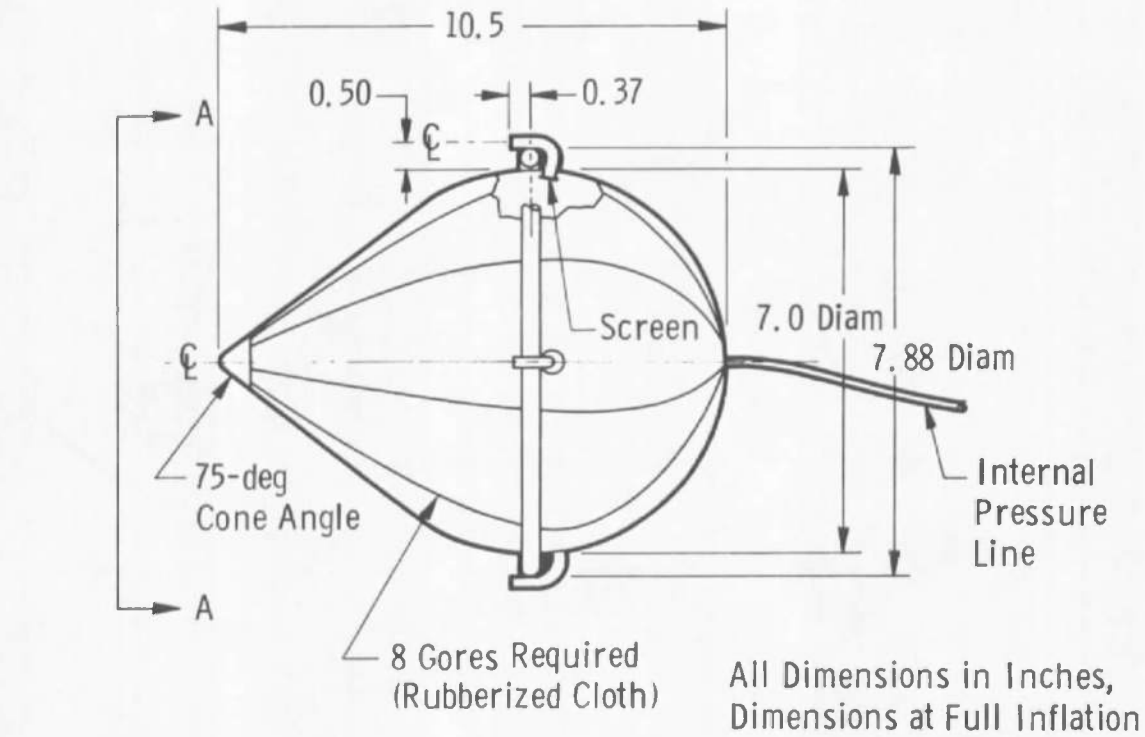

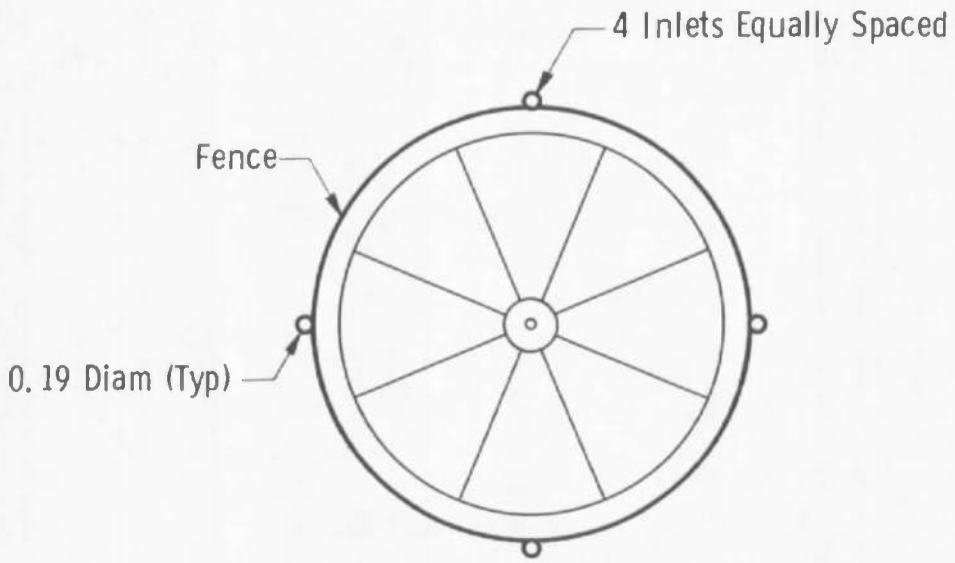

Fig. 7 Sketch of Conical Ballute

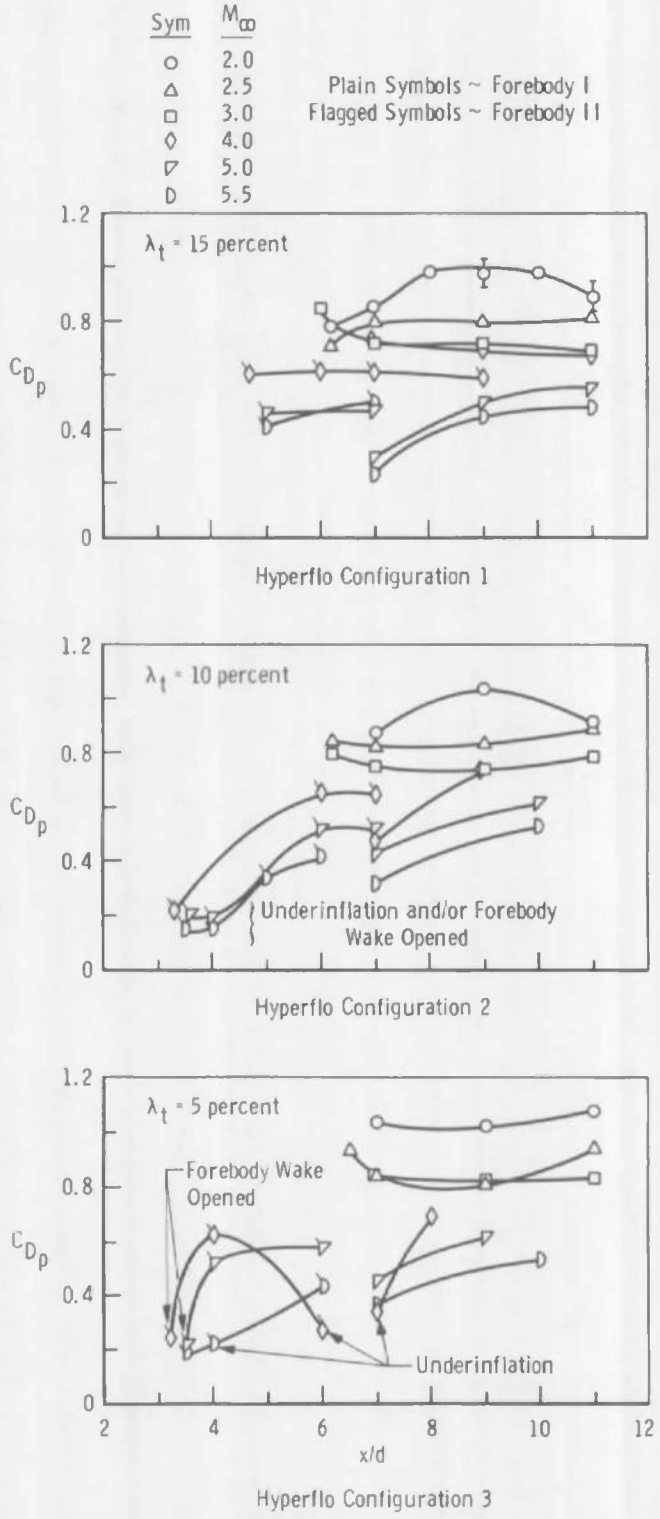

Fig. 8 Variation of Drag Coefficients with Downstream Canopy Location for Hyperflo Parachute Configurations 1, 2, and 3, M_∞ = 2 to 5.5, q_∞ = 1.0 psia

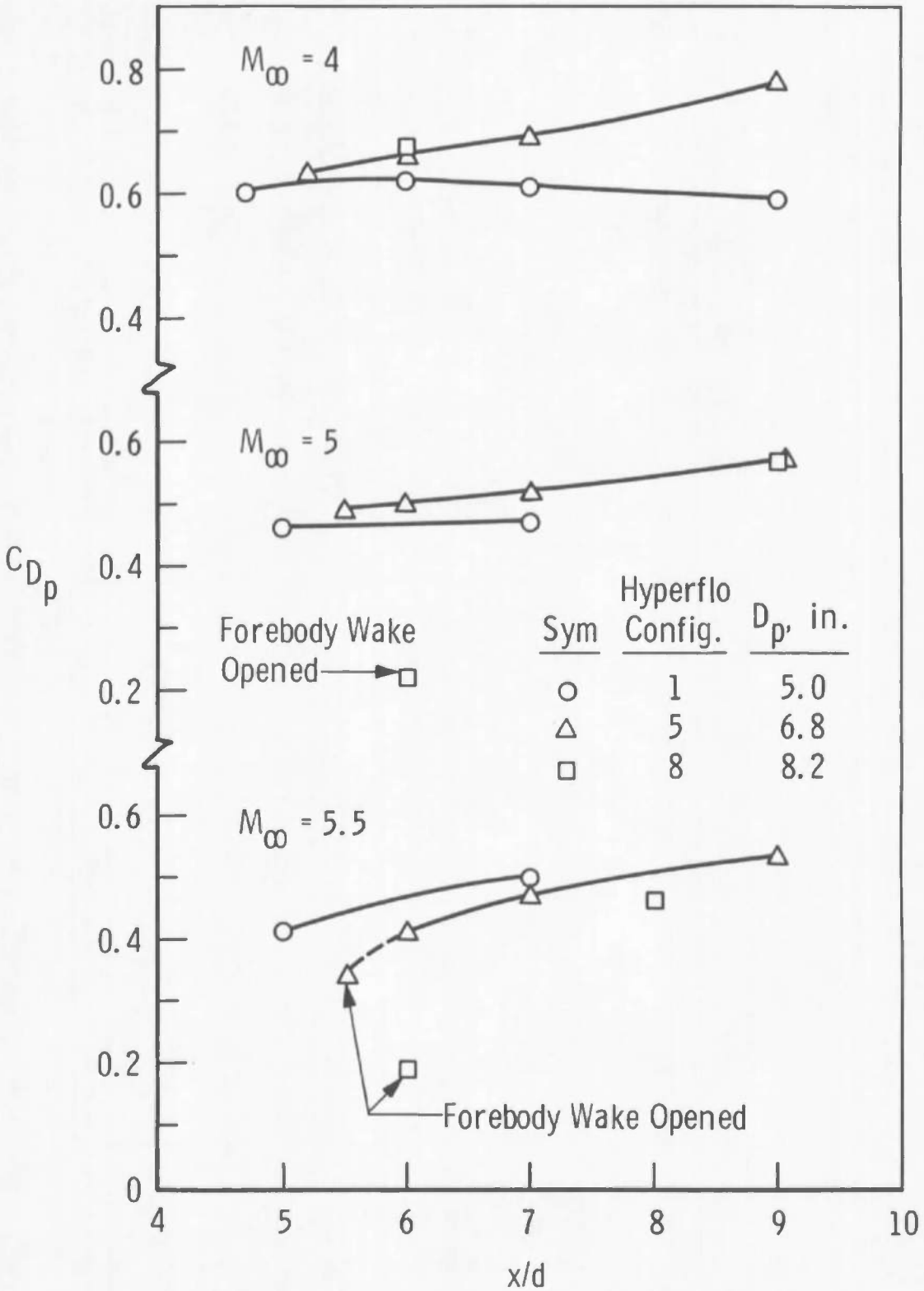

Fig. 9 Effect of Canopy Size on the Drag Characteristics of the Perlon Mesh-Roofed Hyperflo Parachutes of 15-percent Total Porosity, M_∞ = 4 to 5.5, q_∞ = 1.0 psia, Forebody II

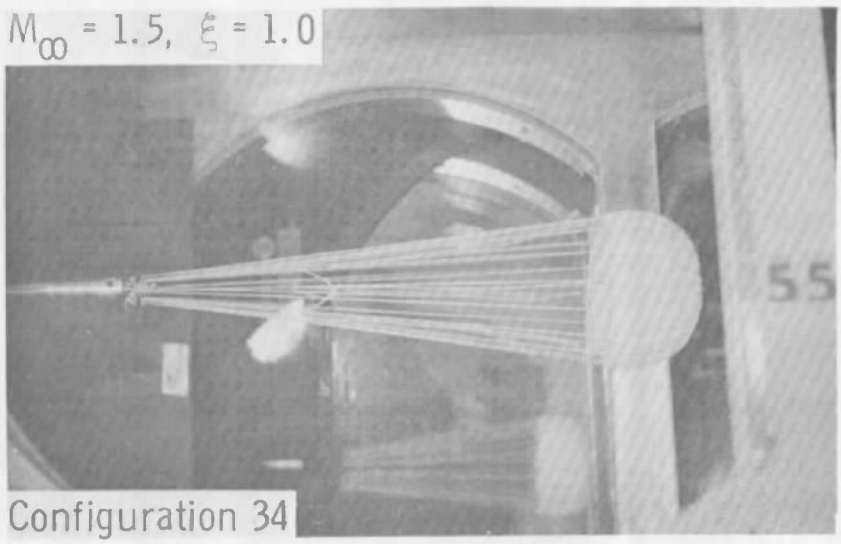

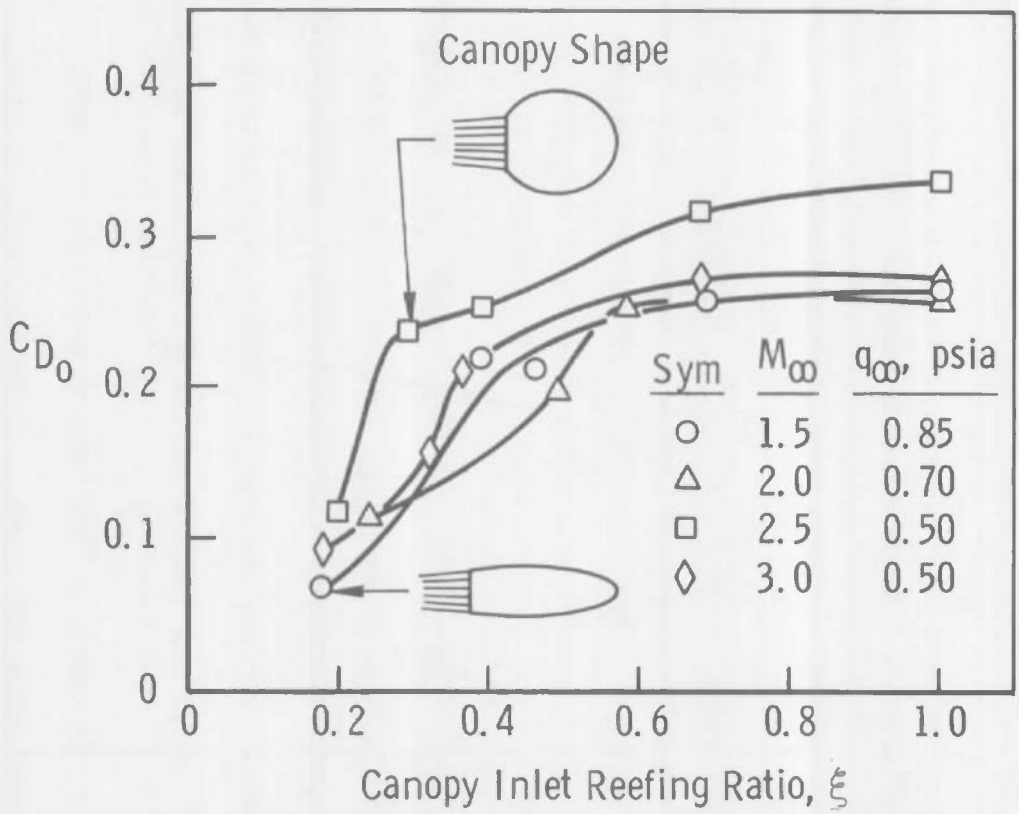

Fig. 10 Effect of Reefing Variation on the Drag Coefficients of 13-in.-diam Hemisfla Parachutes at M_∞ = 1.5 to 3

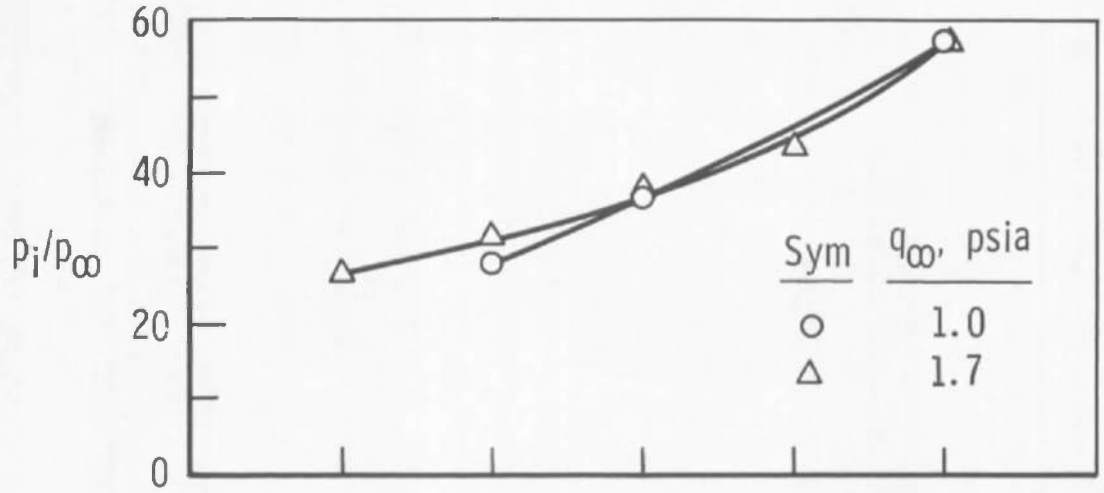

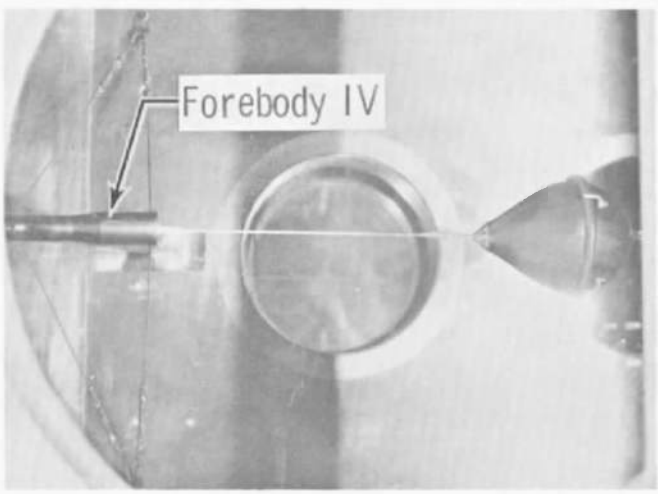

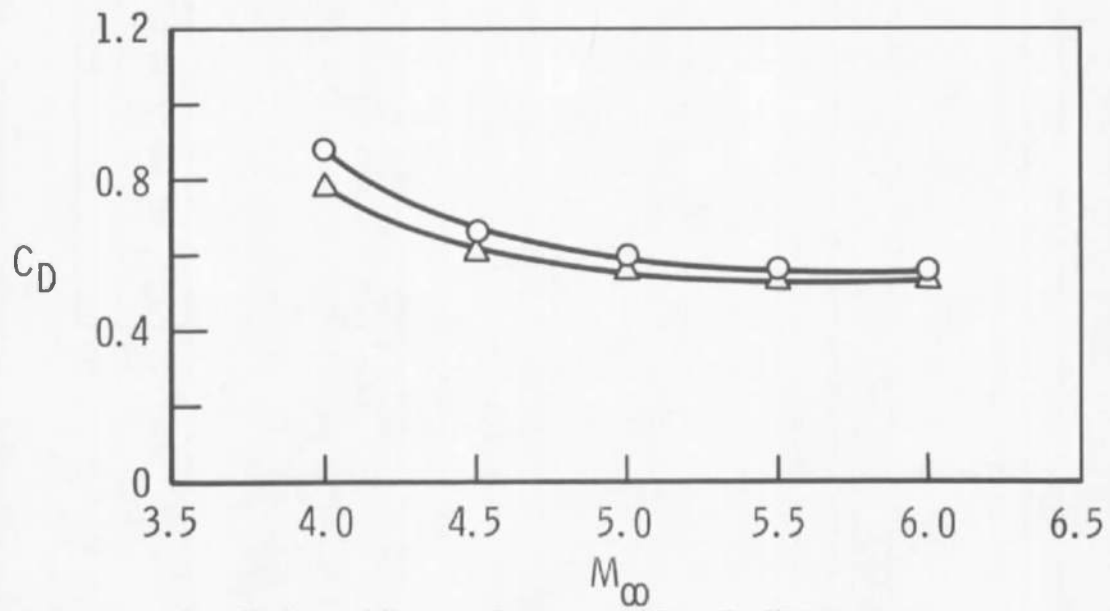

Fig. 11 Internal Pressure Recovery and Drag Coefficient versus Mach Number for the Conical Ballute

TABLE I
HYPERFLO PARACHUTE TEST CONDITIONS AND RESULTS

Parachute Configuration	M_∞	Forebody	x/d		q_∞, psia	C_{Dp}		Remarks
			min.	max.		min.	max.	
1	2.0	I	6.2	16.0	1.0	0.80	1.00	Good inflation at all x/d's, very stable at x/d's < 8; large oscillations (unstable) at x/d > 14
	2.5	I	6.2	11.0	1.0	0.70	0.80	Very stable at x/d = 6.2; slight rocking motion of canopy and small oscillations (±3 deg) at x/d = 9; unstable at x/d = 11
	3.0	I	6.0	11.0	0.5, 0.7, 1.0	0.60	0.85	Good inflation at all conditions; oscillations of ±5 deg at x/d's < 7, q_∞ = 1.0 psia; good stability at x/d's < 9, q_∞ = 0.5 psia
	4.0	I	7.0	11.0	1.0	0.65	0.70	Good inflation at all x/d's; small oscillations at x/d = 7; increased oscillations (±5 deg) at x/d = 9 and 11
	5.0	I	7.0	11.0	1.0	0.30	0.55	Very stable at x/d = 7; good inflation with oscillations of ±5 deg at x/d = 11
	5.5	I	7.0	11.0	1.0	0.25	0.50	Underinflation at all x/d's, no oscillations at x/d = 7
	4.0	II	4.7	9.0	1.0	0.59	0.62	Good inflation at all x/d's; very stable at x/d = 4.7, oscillations at larger x/d's increasing to ±10 deg at x/d = 9
	5.0	II	5.0	7.0	1.0	0.46	0.47	Good inflation; slight rocking motion at x/d = 5; and periodic oscillations (±5 to 10 deg) at x/d = 7
	5.5	II	5.0	7.0	1.0	0.40	0.50	Good inflation; fair stability at x/d = 5; large oscillations (>15 deg) at x/d = 7
2	2.0	I	7.0	11.0	1.0	0.90	1.05	Good inflation at all x/d's; very stable at x/d = 7; slight rocking motion at x/d = 9; periodic oscillations (±5 deg) at x/d = 11
	2.5	I	6.2	11.0	1.0	0.80	0.90	Good inflation at all x/d's; oscillations increased from ±1 deg at x/d = 6.2 to ±5 to 10 deg at x/d = 11
	3.0	I	6.2	11.0	0.5, 0.8, 1.0	0.50	0.90	Generally good inflation; periodic large oscillations (±10 to 15 deg) at x/d's > 7, q_∞ = 1.0 psia; good stability to x/d = 9, q_∞ = 0.5 psia
	4.0	I	7.0	9.0	0.5	0.45	0.75	Rapid rotation and good inflation at x/d = 7; high-frequency oscillations at x/d = 9
	5.0	I	7.0	10.0	0.5	0.40	0.60	Good inflation; spinning at x/d = 7; slight underinflation and oscillation at x/d = 10
	5.5	I	7.0	10.0	0.5	0.30	0.55	Steady but underinflated at x/d = 7; good inflation but high-frequency oscillations (±10 deg) at x/d = 10
	4.0	II	3.3	7.0	1.0	0.20	0.65	Periodic spinning then underinflation at x/d = 3.3; good inflation at x/d = 6 and 7 but large oscillations (10 to 15 deg)
	5.0	II	3.6	7.0	1.0	0.20	0.50	Stable, but inlet underinflated at x/d = 3.6 and 4; good inflation at x/d = 6 and 7, but very unstable beyond x/d = 7
	5.5	II	3.5	6.0	1.0	0.15	0.40	Fair to good inflation at all x/d's; stable at x/d = 3.5 and 4 (rapid spinning at 3.5); small oscillations at x/d = 5 and 6
3	2.0	I	7.0	11.0	1.0	1.00	1.05	Good inflation at all x/d's, periodic oscillation in swivel area increased with x/d
	2.5	I	6.5	11.0	1.0	0.80	0.95	Good inflation at all x/d's; low-frequency oscillations at x/d = 6.5 and 7, rapid swivel oscillations at larger x/d's
	3.0	I	7.0	11.0	1.0	0.80	0.85	Good inflation at all x/d's, oscillations of ±20 deg at all x/d's
	4.0	I	7.0	8.0	0.5	0.35	0.70	Rapid spinning with fair inflation at x/d = 7; good inflation with high-frequency oscillations at x/d = 8
	5.0	I	7.0	9.0	0.5	0.50	0.80	Good inflation and spinning at x/d = 7; periodic oscillations then spinning at x/d = 9
	5.5	I	7.0	10.0	0.5	0.35	0.55	Good inflation, stable at x/d = 7, unstable at x/d = 10
	4.0	II	3.2	6.0	1.0	0.25	0.60	Stable but underinflated below x/d = 4; fair inflation but oscillations of ±10 deg at x/d = 6

TABLE I (Continued)

Parachute Configuration	M_∞	Forebody	x/d		q_∞, psia	C_{D_p}		Remarks
			min.	max.		min.	max.	
3	5.0	II	3.5	9.0	1.0	0.20	0.55	Stable and underinflated at x/d = 3.5 and 4; good inflation but oscillations (±10 deg) at larger x/d's
	5.5	II	3.5	6.0	1.0	0.20	0.45	Fair inflation at x/d = 3.5 and 4; rapid spinning at x/d = 3.5; good inflation with 5- to 7-deg oscillations at x/d = 6.
4	2.0	I	6.4	7.0	1.0	0.70	0.90	Good inflation; very stable at x/d = 6.4; violently unstable at x/d = 7
5	4.0	II	5.2	9.0	1.0	0.60	0.80	Good inflation at all x/d's; periodic oscillations of ±3 deg at x/d = 5.2 increased to ±15 deg at x/d = 9
	5.0	II	5.5	9.0	1.0	0.50	0.60	Good inflation, high-frequency oscillations of ±5 to 7 deg at all x/d's
	5.5	II	5.5	9.0	1.0	0.35	0.50	Stable at x/d = 5.5; oscillations of ±5 to 7 deg and good inflation at x/d = 7 and 9
8	4.0	II	6.0		1.0	0.67		Good inflation, oscillations of ±5 deg
	5.0	II	6.0	9.0	1.0	0.20	0.60	Good inflation, stable but high spin rate at x/d = 6; high-frequency oscillations (±10 deg) at x/d = 9
	5.5	II	6.0	8.0	1.0	0.20	0.45	Good inflation, stable with rapid spinning at x/d = 6; oscillations of ±5 deg at x/d = 8
	4.0	III	4.3	6.0	0.5	0.30	0.40	Good inflation at all x/d's; small oscillations increased slightly with increasing x/d
	5.0	III	4.3	6.0	0.5	0.25	0.30	Similar in performance to that at M_∞ = 4
	5.5	III	4.3	6.0	0.5	0.25	0.30	Similar in performance to that at M_∞ = 4
9	4.0	II	5.8	7.0	0.5	0.50	1.00	Good inflation with rapid spinning and small oscillations at x/d = 5.8; very unstable at x/d = 7
	5.0	II	5.8	7.0	0.5	0.40	0.60	Same as at M_∞ = 4
	5.5	II	6.0	7.0	0.5	0.35	0.55	Same as at M_∞ = 4
	4.0	III	4.2	6.0	0.5	0.50	0.60	Good inflation, periodic oscillations (±5 deg) and stability at x/d = 4.2, unstable at x/d = 6
10	4.0	II	5.5	6.0	0.5	0.30	0.35	Fair stability with underinflation at x/d = 5.5; well inflated but unstable at x/d = 6
	5.0	II	5.5	7.0	0.5	0.25	0.60	Same as at M_∞ = 4
	5.5	II	5.5	8.0	0.5	0.15	0.50	Fair stability with underinflation at x/d = 5.5 and 6; oscillations of ±10 deg at x/d = 8
13	4.0	II	6.0	9.0	0.5	0.30	0.90	Very stable and underinflated at x/d = 6; good inflation but large oscillations (±30 deg) at x/d = 9
	5.0	II	6.0	9.0	0.5	0.25	0.60	Same as at M_∞ = 4
	5.5	II	6.0	9.0	0.5	0.20	0.50	Same as at M_∞ = 4
14	4.0	II	6.0	7.0	1.0	0.18		Stable and underinflated at x/d = 6; lost model when at x/d = 7
15	4.0	II	5.5	7.0	0.5	0.25	0.75	Stable but underinflated at x/d = 5.5; oscillations of ±20 deg at x/d = 7
	5.0	II	5.5	8.0	0.5	0.25	0.45	Better inflation at x/d = 5.5 than at M_∞ = 4; oscillations increased with x/d; very unstable at x/d = 8
	5.5	II	5.5	8.0	0.5	0.15	0.60	Same as at M_∞ = 5 with a little better inflation characteristics

TABLE I (Concluded)

Parachute Configuration	M_∞	Forebody	x/d min.	x/d max.	q_∞, psia	C_{D_p} min.	C_{D_p} max.	Remarks
17	2.0	I	7.3		1.0	1.00		Unstable, oscillations of ±30 deg
	3.0	I	7.3	11.0	1.0	0.80	0.85	Good inflation; unstable; oscillations of ±20 deg at all x/d's
	4.0	II	3.5	6.0	0.5	0.25	0.70	Good inflation at all x/d's; stable but spinning rapidly at x/d = 3.5; periodic oscillations and rotations at x/d = 6
	5.0	II	3.5	6.0	0.5	0.20	0.50	Good inflation, spinning with oscillation at swivel at x/d = 3.5; periodic oscillation and spinning at x/d = 6
	5.5	II	3.5	6.0	0.5	0.20	0.45	Similar characteristics as at M_∞ = 4
18	2.0	I	7.0	9.0	1.0	0.95	1.00	Fair stability at x/d = 7 but very unstable at x/d's > 8
	2.5	I	6.5	0.0	1.0	0.85	0.90	Unstable; some underinflation at x/d = 6.5
	3.0	I	6.5	9.0	1.0	0.75	0.80	Unstable
	4.0	I	6.8	11.0	0.5	0.30	0.80	Stable with fair inflation at x/d = 6.8; good inflation but unstable at x/d's > 8
	5.0	I	7.0	9.0	0.5	0.30	0.60	Very stable but underinflated at x/d = 7; good inflation with periodic oscillations (±10 deg) at x/d = 9
	5.5	I	7.0	11.0	0.5	0.25	0.50	Same as at M_∞ = 5
	4.0	II	3.0	7.0	0.5	0.30	0.70	Stable with a tendency to spin at x/d = 3; good inflation but large oscillations at x/d = 5 and 7
	5.0	II	3.0	5.0	0.5	0.10	0.55	Good inflation and stable but spinning rapidly at x/d = 3; unstable at x/d = 5
19	4.0	II	3.5	5.0	0.8	0.20	0.50	Good inflation; rapid spinning but stable at x/d = 3.5; unstable at x/d = 5
	5.0	II	3.5	6.0	0.5	0.25	0.60	Same as at M_∞ = 4
	5.5	II	3.5	5.0	0.5	0.20	0.30	Same as at M_∞ = 4 and spinning at x/d = 5
	4.0	III	3.5	4.0	0.5	0.35	0.40	Fair stability, low-amplitude oscillations; very unstable beyond x/d = 4.5
	5.0	III	3.5		0.5	0.40		Good inflations but large oscillations (±20 deg)
21	2.0	I	6.5	9.0	1.0	0.70	0.95	Very stable at x/d = 6.5; stable (some low-amplitude oscillations) at x/d = 7.5; unstable at x/d = 8.2 and 9
	2.5	I	6.5	11.0	1.0	0.75	0.90	Same as at M_∞ = 2; periodic violent instability at x/d = 11
	3.0	I	6.5	9.0	1.0	0.70	0.80	Unstable, periodic oscillations
22	4.0	I	6.1	8.0	0.5	0.50	0.90	Good inflation at all x/d's; stable at x/d = 6.1 and 7 and spinning at x/d = 7
	5.0	I	7.0	9.0	0.5	0.30	0.65	Same as at M_∞ = 4
	5.5	I	7.0	10.0	0.5	0.35	0.70	Same as at M_∞ = 4

See Fig. 4 for hyperflo parachute specifications.

TABLE II
HEMISFLO PARACHUTE TEST CONDITIONS AND RESULTS

Parachute Configuration	M_∞	Forebody	x/d	ξ min.	ξ max.	q_∞, psia	C_{D_0} min.	C_{D_0} max.	Remarks
31	2.0	I	19.5	0.08	0.38	0.7	0.06	0.11	Squidding at all reefing ratios; oscillations did not exceed ±2 deg; poor inflation at ξ = 0.08
	2.5	I	19.5	0.12	0.29	0.5	0.05	0.25	Same as at M_∞ = 2; oscillations of ±3 to 5 at ξ = 0.29
	3.0	I	19.5	0.075	0.26	0.5	0.04	0.17	Squidding at all reefing ratios; oscillations of ±5 deg at ξ = 0.26 and slightly larger at ξ = 0.25
32	2.0	I	19.5	0.085	0.38	0.7	0.05	0.14	Similar to Config. 31 at M_∞ = 2; poor canopy inflation at ξ = 0.085; good inflation at ξ = 0.25 and 0.38
	2.5	I	19.5	0.08	0.31	0.5	0.03	0.14	Same as M_∞ = 2, fair inflation at ξ = 0.18 and above
	3.0	I	19.5	0.08	0.33	0.5	0.03	0.14	Squidding at all reefing ratios; fair inflation at ξ = 0.20 and above; oscillations (±5 deg) at ξ = 0.22
33	1.5	I	19.5	0.10		0.8	0.03		Canopy squidding (poor inflation); rapid vibration of suspension lines
	2.0	I	19.5	0.08	0.22	0.7	0.03	0.09	Canopy squidding, underinflated at ξ = 0.08; fair inflation with ±2 deg oscillations at ξ = 0.22
	2.5	I	19.5	0.08	0.28	0.5	0.03	0.13	Squidding at all reefing ratios; good stability at ξ = 0.08 and 0.12; line vibrations at ξ = 0.28
	3.0	I	19.5	0.08	0.24	0.5	0.03	0.12	Better inflation at ξ = 0.08 than at other Mach numbers; overall fair inflation without oscillations
34	1.5	I	11.0	0.18	1.00	0.8	0.07	0.28	Canopy squidding and oscillation of ±1 deg at ξ = 0.18; excellent inflation and stability at ξ = 0.39 to 1.0
	2.0	I	11.0	0.23	1.00	0.7, 1.0, 1.5	0.11	0.26	Very good inflatinn and stability at all reefing ratios; slow rotation and oscillation (±1 deg) at ξ = 1.0
	2.5	I	11.0	0.20	1.00	0.5, 0.8, 1.0, 1.5	0.11	0.34	Very good inflation at all reefing ratios; oscillations of ±5 deg occurred at ξ = 0.68 and 1.0
	3.0	I	11.0	0.18	1.00	0.5, 0.8, 1.0, 1.5	0.09	0.27	Very good inflation at all reefing ratios, oscillations occurred at ξ = 0.36; unstable at ξ = 1.0
38	2.0	I	5.5	1.00		0.7	0.24		Unstable, violent pulsing of canopy
	2.5	I	5.5	1.00		0.5	0.20		Unstable, violent pulsing of canopy
	3.0	I	5.5	1.00		0.5	0.16		Much better stability; good inflation with slight squidding tendency; oscillations of ±2 deg

See Fig. 5 for hemisflo parachute specifications.

TABLE III
HYPERFLO-HEMISFLO TANDEM PARACHUTE TEST CONDITIONS AND RESULTS

Parachute Configuration	M_∞	Forebody	q_∞, psia	13-in. D_o Hemisflo			3-in. D_p Hyperflo		Remarks
				x/d	ξ	C_{D_o}	x/d	C_{D_p}	
35 (Hyperflo inside hemisflo suspension lines)	2.0	I	0.7	11	1.0	0.30	4.75	0.52	Good inflation and stability in both parachutes; the hyperflo control line wrapped around three of the hemisflo suspension lines on deployment and the lines remained intertwined throughout the testing.
	2.0	I	0.7	11	1.0	0.35	7.25	0.63	Same characteristics as above
	3.0	I	0.5	11	1.0	0.11	4.00	1.09	As above but with low-amplitude, low-frequency oscillation in the hemisflo
	3.0	I	0.5	11	1.0	0.14	6.50	0.63	Good inflation and stability

See Figs. 4 and 5 for parachute specifications.

TABLE IV
BALLUTE DECELERATOR TEST CONDITIONS AND RESULTS

Configuration	M_∞	Forebody	q_∞, psia	x/d	C_D	Remarks
75-deg conical ballute with a 6.3-percent fence and side inlets	4.0	IV	1.0	9.0	0.88	The ballute model was very stable and well inflated at each Mach number and dynamic pressure level.
		IV	1.7	9.0	0.78	
	4.5	IV	1.0	9.0	0.66	
		IV	1.7	9.0	0.61	
	5.0	IV	1.0	9.0	0.60	
		IV	1.7	9.0	0.56	
	5.5	IV	1.0	9.0	0.56	
		IV	1.7	9.0	0.54	
	6.0	IV	1.0	9.0	0.56	
		IV	1.7	9.0	0.53	

UNCLASSIFIED

Security Classification

DOCUMENT CONTROL DATA - R&D

(Security classification of title, body of abstract and indexing annotation must be entered when the overall report is classified)

1. ORIGINATING ACTIVITY (Corporate author)	2a. REPORT SECURITY CLASSIFICATION
Arnold Engineering Development Center, ARO, Inc., Operating Contractor, Arnold Air Force Station, Tennessee	UNCLASSIFIED
	2b. GROUP N/A

3. REPORT TITLE

WIND TUNNEL INVESTIGATION OF FLEXIBLE AERODYNAMIC DECELERATOR CHARACTERISTICS AT MACH NUMBERS 1.5 TO 6

4. DESCRIPTIVE NOTES (Type of report and inclusive dates)

N/A

5. AUTHOR(S) (Last name, first name, initial)

Deitering, J. S., and Hilliard, E. E., ARO, Inc.

6. REPORT DATE	7a. TOTAL NO. OF PAGES	7b. NO. OF REFS
June 1965	34	None

8a. CONTRACT OR GRANT NO. AF 40(600)-1000	9a. ORIGINATOR'S REPORT NUMBER(S)
b. PROJECT NO. 6065	AEDC-TR-65-110
c. Program Element 62405364	9b. OTHER REPORT NO(S) (Any other numbers that may be assigned this report)
d. Task 606505	N/A

10. AVAILABILITY/LIMITATION NOTICES

Qualified requesters may obtain copies of this report from DDC. DDC release to CFSTI and foreign announcement and distribution of this report are not authorized.

11. SUPPLEMENTARY NOTES	12. SPONSORING MILITARY ACTIVITY
N/A	Air Force Flight Dynamics Laboratory, Air Force Systems Command, Wright-Patterson AF Base, Ohio

13. ABSTRACT

Tests were conducted in the 40-in. supersonic Tunnel A of the von Kármán Gas Dynamics Facility to investigate the drag and stability characteristics of a series of flexible decelerator models. The models were tested at Mach numbers from 1.5 to 6 at dynamic pressures corresponding to pressure altitudes of 75,000 to 135,000 ft, respectively. Four basic decelerator configurations were examined: hyperflo parachutes at variable locations aft of three forebody models, hemisflo parachutes with varied amounts of canopy inlet reefing, a tandem configuration composed of a hyperflo parachute inside the suspension lines of a hemisflo parachute, and a conical ballute decelerator.

This document has been approved for public release and its distribution is unlimited. Per A. F. Letter dtd. 6 October 1971 signed William O. Cole

DD FORM 1 JAN 64 1473

UNCLASSIFIED

Security Classification

14 KEY WORDS	LINK A ROLE	LINK A WT	LINK B ROLE	LINK B WT	LINK C ROLE	LINK C WT
parachutes						
deceleration						
supersonic flow						
drag						
stability						
hyperflo						
hemisflo						
ballute						
tandem						

INSTRUCTIONS

1. ORIGINATING ACTIVITY: Enter the name and address of the contractor, subcontractor, grantee, Department of Defense activity or other organization *(corporate author)* issuing the report.

2*a*. REPORT SECURITY CLASSIFICATION: Enter the overall security classification of the report. Indicate whether "Restricted Data" is included. Marking is to be in accordance with appropriate security regulations.

2*b*. GROUP: Automatic downgrading is specified in DoD Directive 5200.10 and Armed Forces Industrial Manual. Enter the group number. Also, when applicable, show that optional markings have been used for Group 3 and Group 4 as authorized.

3. REPORT TITLE: Enter the complete report title in all capital letters. Titles in all cases should be unclassified. If a meaningful title cannot be selected without classification, show title classification in all capitals in parenthesis immediately following the title.

4. DESCRIPTIVE NOTES: If appropriate, enter the type of report, e.g., interim, progress, summary, annual, or final. Give the inclusive dates when a specific reporting period is covered.

5. AUTHOR(S): Enter the name(s) of author(s) as shown on or in the report. Enter last name, first name, middle initial. If military, show rank and branch of service. The name of the principal author is an absolute minimum requirement.

6. REPORT DATE: Enter the date of the report as day, month, year, or month, year. If more than one date appears on the report, use date of publication.

7*a*. TOTAL NUMBER OF PAGES: The total page count should follow normal pagination procedures, i.e., enter the number of pages containing information.

7*b*. NUMBER OF REFERENCES: Enter the total number of references cited in the report.

8*a*. CONTRACT OR GRANT NUMBER: If appropriate, enter the applicable number of the contract or grant under which the report was written.

8*b*, 8*c*, & 8*d*. PROJECT NUMBER: Enter the appropriate military department identification, such as project number, subproject number, system numbers, task number, etc.

9*a*. ORIGINATOR'S REPORT NUMBER(S): Enter the official report number by which the document will be identified and controlled by the originating activity. This number must be unique to this report.

9*b*. OTHER REPORT NUMBER(S): If the report has been assigned any other report numbers *(either by the originator or by the sponsor)*, also enter this number(s).

10. AVAILABILITY/LIMITATION NOTICES: Enter any limitations on further dissemination of the report, other than those imposed by security classification, using standard statements such as:

(1) "Qualified requesters may obtain copies of this report from DDC."

(2) "Foreign announcement and dissemination of this report by DDC is not authorized."

(3) "U. S. Government agencies may obtain copies of this report directly from DDC. Other qualified DDC users shall request through _____."

(4) "U. S. military agencies may obtain copies of this report directly from DDC. Other qualified users shall request through _____."

(5) "All distribution of this report is controlled. Qualified DDC users shall request through _____."

If the report has been furnished to the Office of Technical Services, Department of Commerce, for sale to the public, indicate this fact and enter the price, if known.

11. SUPPLEMENTARY NOTES: Use for additional explanatory notes.

12. SPONSORING MILITARY ACTIVITY: Enter the name of the departmental project office or laboratory sponsoring *(paying for)* the research and development. Include address.

13. ABSTRACT: Enter an abstract giving a brief and factual summary of the document indicative of the report, even though it may also appear elsewhere in the body of the technical report. If additional space is required, a continuation sheet shall be attached.

It is highly desirable that the abstract of classified reports be unclassified. Each paragraph of the abstract shall end with an indication of the military security classification of the information in the paragraph, represented as *(TS)*, *(S)*, *(C)*, or *(U)*.

There is no limitation on the length of the abstract. However, the suggested length is from 150 to 225 words.

14. KEY WORDS: Key words are technically meaningful terms or short phrases that characterize a report and may be used as index entries for cataloging the report. Key words must be selected so that no security classification is required. Identifiers, such as equipment model designation, trade name, military project code name, geographic location, may be used as key words but will be followed by an indication of technical context. The assignment of links, rules, and weights is optional.